High Power 1.5 µm Pulsed Semiconductor Laser Design with a Bulk Active Layer and an Asymmetric Waveguide

Boris S. Ryvkin[1,2], Eugene A. Avrutin[3*], *Member, IEEE,* Lauri W. Hallman[1], and Juha T. Kostamovaara[1], *Senior Member, IEEE*

[1] *Dept of Electrical and Information Engineering, University of Oulu, Oulu, Finland*

[2] *A. F. Ioffe Physico-Technical Institute, St. Petersburg 194021, Russia*

[3] *Dept of Electronic Engineering, University of York, York, UK*

** Tel.+44-1904-322341; Fax+44-1904-322335; e-mail: eugene.avrutin@york.ac.uk*

ABSTRACT

InGaAsP/InP high pulsed power lasers operating in the range of 1.3 – 1.6 µm have been intensely studied recently, with LIDAR technology being the primary application. We present and analyse a design with a bulk active layer which has a large refractive index step with respect to the optical confinement layer and is located close to the *p*-cladding. It is shown that such lasers can allow a noticeable performance increase over the state of the art. The dependence of the laser performance on the design parameters including the thicknesses of the active layer and the waveguide, the cavity length, and the waveguide asymmetry, is analysed. It is shown that short cavity lengths (~1 mm or even shorter) can be used in the design considered for achieving high pulsed power. Due to the significant waveguiding properties of the active layer, the use of both symmetric and asymmetric waveguide designs is possible, with only slightly higher output predicted for the asymmetric one. Both designs allow operation with a single, broad transverse mode enabling high brightness.

Keywords: semiconductor lasers, high-power lasers, eye safe lasers, laser efficiency.

1. INTRODUCTION

There has been considerable effort in the recent years aimed at improving the performance (output power and brightness) of broad area pulsed diode lasers operating in the eye-safe spectral range (λ~ 1400 – 1700 nm) for applications ranging from medical instrumentation to range finding / LIDAR systems [1]. Several device designs have been proposed, with the aim of ensuring high output efficiency for all operating currents, for which keeping the internal optical losses as low as possible at all currents is crucial. The common feature of these designs is the small thickness $l_{p\text{-OCL}}$ of the *p*-side of the Optical Confinement Layer (OCL), which helps minimising the losses caused by spatially non-uniform accumulation of holes in the *p*-OCL at high injection levels, identified in our early papers [2] as the major source of losses at high pulsed power. The two major design types with a narrow *p*-OCL that have been used in eye-safe lasers are the ultra-narrow waveguide [3],[4] and the broad asymmetric waveguide designs [5]. The latter design, which was used in our work among others, has the advantage of allowing the use of highly doped *p*-cladding layers thus minimising the electric resistance and electron leakage without significant compromise to optical losses. Nearly all high-power laser diode structures used at any wavelength so far have used active layers (ALs) consisting of only a few (1-3) Quantum Wells (QWs) and thus very weakly affecting the waveguiding properties of the laser structure. This necessitated the use of complex double-and triple-asymmetric waveguide structures, sometimes with graded index layers, for optimisation of the laser performance [6],[7]. In our approach, we have made use of the fact that the technology of (lattice matched) InGaAsP/InP (or AlGaInAs/InP) family materials used in eye-safe lasers allows fabrication of broad, bulk active layers with substantial waveguiding properties of their own, and demonstrated their use for eye-safe asymmetric waveguide lasers [8]-[11]. An additional decrease in optical losses in eye-safe lasers was shown to be achievable from highly doping the *n*- side of the OCL [8]. This paper summarises the experimental and theoretical work so far, discusses the possibilities of this laser design, and briefly points out some advantages of lasers with bulk active layers over those using Multiple Quantum Wells (MQW).

2. LASER STRUCTURES, THEORETICAL APPROACH AND RESULTS

A typical laser structure we have been using is shown in Fig. 1 and is a double-asymmetric (AL position and refractive index steps) rectangular waveguide structure with a broad active layer. The *n*-side of the OCL (and the *p*-cladding) are assumed to be strongly doped to minimise the resistance, the carrier accumulation in the *n*-OCL, and the carrier leakage into the *p*-cladding. The parameters fixed in the studies below are the refractive index steps ($\Delta n_{act} \approx 0.27$, and $\Delta n_p \approx 0.064$ [8]-[11], and the thicknesses of *n*-OCL layer ($l_{n\text{-OCL}}$ =1.8 µm as in [9],[10] or 2.8 µm as in [8]). The parameters that can be varied are the refractive index step at the *n*-OCL/*n*-cladding interface Δn_n and the width of the active layer *d*, taken to be $d = 600$ Å in the figure. A stripe 100 µm wide is assumed throughout the calculations. The mirror reflectances are taken as asymmetric ($R_1 = 0.95$, $R_2 = 0.05$), and

the laser resonator length L is varied between 0.5 and 2 mm, leading to a variation in the outcoupling losses $\alpha_{out} = 1/L \times \ln\left(1/(R_1 R_2)\right)$.

Figure 2 shows that the waveguiding properties of the active layer are quite important for the waveguiding in the laser: the mode is largely attracted to the active layer. This is reflected in the strong and markedly nonlinear increase in the confinement factor Γ of the fundamental mode with the active layer thickness d, shown in Fig. 2; the figure also shows that the waveguiding properties of the active layer are to a large extent responsible for strong fundamental mode selection. The final linear parameter of the laser structure is the built-in absorption $\alpha_{in}^{built-in}$ formed mainly by the free hole absorption in the moderately doped p-OCL and highly doped p-cladding and determined in its turn by the modal structure and the free carrier absorption cross-section $\sigma_{fc} = \sigma_e + \sigma_h \approx \sigma_h$, ($\sigma_h = 4\times10^{-17}$ cm^2 [13],[14] and $\sigma_e << \sigma_h$ being free electron and hole absorption cross section). The values of Γ, $\alpha_{in}^{built-in}$, and α_{out}, together with the gain cross-section $\sigma_g = 3.13\times10^{-16}$ cm^2 [15] determine the threshold carrier density $N_{th} = \dfrac{\alpha_{in}^{built-in} + \alpha_{out} + \Gamma\sigma_g N_{tr}}{\Gamma\left[\sigma_g - \sigma_{fc}\right]}$ also shown in Fig. 2. The value decreases strongly with d at small active layer thicknesses, but beyond the value of $d = 600$ Å as shown in Fig. 1, further decrease is gentle, which was one of the reasons for the choice of the value $d = 600$ Å.

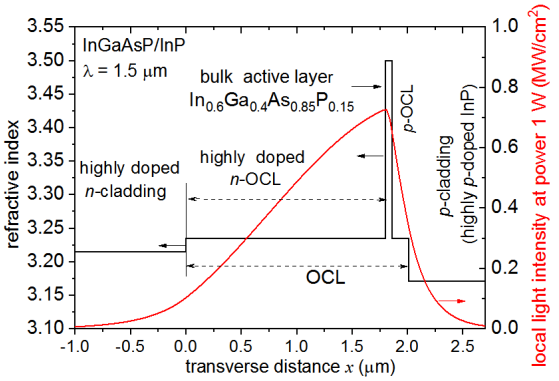

Figure 1. Schematic of the laser structure and the waveguide mode intensity distributions for waveguides with the Active Layer thickness d = 600 Å.

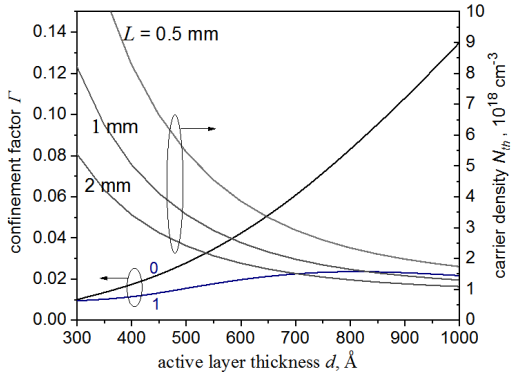

Figure 2. Confinement factor Γ for the fundamental mode (0) and the higher order mode nearest to excitation (1) and N_{th} as functions of d. All other waveguide parameters as in Fig. 1.

Through the paper, following we consider pulsed (quasi-CW) operating regime, with the injection current pulse duration << 100 ns as is the case in LIDAR applications, so room temperature operation is assumed throughout. For the values of L and $R_{1,2}$ used, a lumped model can be used to analyse the output power with sufficient accuracy. The output power P is then calculated as function of injection current I using the transcendental equation

$$P(I) = \eta_i \frac{\hbar\omega}{e} \frac{\alpha_{out}}{\alpha_{out} + \alpha_{in}(I, P(I))} \left(I - I_{th}(I)\right) \tag{1}$$

Here the effective threshold current $I_{th}(I)$ is the current expended on creating the active layer carrier density necessary for the gain to compensate the total losses $\alpha_{out} + \alpha_{in}(I, P(I))$. The injection efficiency is taken as η_i=1. The internal loss (absorption) coefficient in the laser is calculated as

$$\alpha_{in}(I, P(I)) \approx \alpha_{in}^{(\text{built-in})} + \alpha_{active}^{(\text{FC})}(I) + \alpha_j^{(\text{FC})}(I) + \alpha_{TPA}^{(\text{FC})}(P(I)) + \alpha_{TPA}^{(\text{mod})}(P(I)) \tag{2}$$

These, as in [8]-[11], are the built-in optical losses $\alpha_{in}^{(\text{built-in})}$, the free hole absorption in the active layer $\alpha_{active}^{(\text{FC})}(I)$, the loss $\alpha_j^{(\text{FC})}(I)$ due to current-induced carrier accumulation in the OCL (in the current design with active layer located very near the p-cladding, this affects mainly the n-OCL), and the direct $\alpha_{TPA}^{(\text{mod})}(P(I))$ and indirect $\alpha_{TPA}^{(\text{FC})}(P(I))$ contributions of the two-photon absorption (TPA) [8],[12]. The TPA coefficient $\beta_{2,OCL} = 6\times10^{-8}$ cm/W of the InGaAsP OCL material significantly exceeds the corresponding value in AlGaAs materials, making the TPA effect particularly important to consider in eye-safe wavelength range lasers. The calculations are performed self-consistently while calculating the output power P [8]-[11]. The calculated values are shown in Fig. 3, alongside the total loss $\alpha_{in}(I, P(I))$, as functions of current I for a 1 mm long laser cavity. As in previous work, the current-induced carrier contribution $\alpha_j^{(\text{FC})}(I)$ is strongly suppressed: the p-OCL contribution mainly by the asymmetric active layer position and the n-OCL contribution by the high n-OCL doping. The direct TPA effect is also very weak. This leaves the indirect effect $\alpha_{TPA}^{(\text{FC})}(P(I))$ as the main reason of

the increase in $\alpha_{in}(I,P(I))$ with current in this material and laser design, though this effect, too, is partly suppressed by the recombination of the TPA-generated carriers in the highly doped *n*-OCL [8]. Figure 4 shows the calculated light-current curves for lasers with three cavity lengths (L = 0.5 mm, 1 mm and L = 2 mm), for two thicknesses of the *n*-OCL ($l_{n\text{-OCL}}$ = 1.8 μm and 2.8 μm). Lasers with shorter cavities (higher α_{out}) give higher output powers at high injection levels. This is made possible by the use of a structure with a small $l_{p\text{-}OCL}$ in which $\alpha_j^{(FC)}(I)$, governed by the *current density*, is suppressed, and so the strong internal losses in short cavities at high currents can be avoided at room temperature. The power values predicted, for the stripe width considered (w = 100 μm), room temperature operation, and high injection level (I ~ 100 A), promise a substantial step forward compared to published results**.**

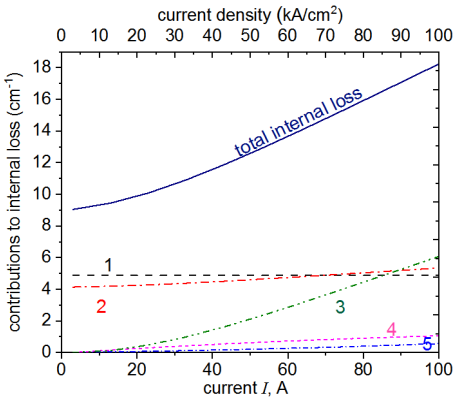

Figure 3. Calculated total internal loss and its components as functions of I: $\alpha_{in}^{(built-in)}$ (1), $\alpha_{active}^{(FC)}(I)$ (2), $\alpha_{TPA}^{(FC)}(P(I))$ (3), $\alpha_{TPA}^{(mod)}(P(I))$ (4), $\alpha_j^{(FC)}(I)$ (5). L= 1 mm, Waveguide parameters as in Fig. 1

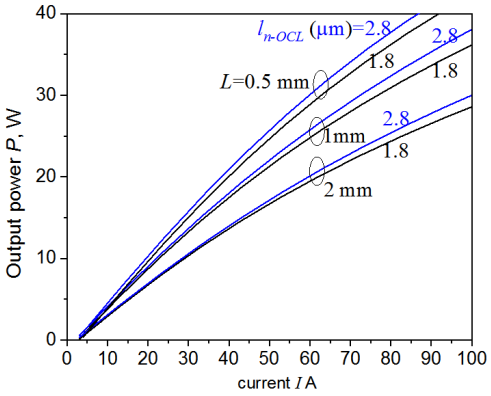

Figure 4. Calculated output power for different values cavity parameters. The active layer thickness is d = 600 Å for $l_{n\text{-}OCL}$=1.8 μm and d = 700 Å for $l_{n\text{-}OCL}$=2.8 μm, the rest of the laser parameters as in Fig. 1

3. EXPERIMENTAL RESULTS

The structure similar to that of Fig. 1, with $l_{n\text{-OCL}}$ = 1.8 μm, was realised in the recent studies [9]-[10]. The results, measured from as-cleaved lasers under current pulses ~ 60 ns long and kHz repetition frequencies, are shown in Fig. 5 for two laser cavity lengths. Output powers of ~ 18 W have been measured at I~ 80 A (Fig. 5).

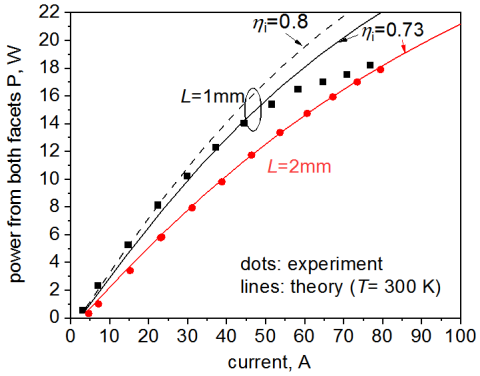

Figure 5. Simulated and experimental output curves from as-cleaved lasers for two cavity lengths.

Despite the relatively low η_i = 0.73 estimated from experiment (and setting one of the performance limitations), the results are comparable with the state of the art for similar wavelength, laser cavity parameters, and current range. The measured performance of lasers with L = 2 mm agrees well with room-temperature simulations. For lasers with L = 1 mm, performance superior to that of longer lasers is observed at moderate currents; at I > 30 – 50 A (depending on the η_i value used in simulations), the measured curve saturation is somewhat stronger than the simulated; this is likely to be due to residual current heating and should be improved by optimised laser mounting (the experiment used *p*-side up mounting using silver epoxy glue).

4. BULK VERSUS MQW ACTIVE LAYERS

Finally, we present some preliminary comparison of the simulated performance of the laser with a bulk AL as shown in Fig. 1 with an identical structure employing an InGaAs MQW AL with the same overall (QWs plus barriers) thickness (a substantially larger number of wells appears to be impractical due to potential problems

with non-equal well populations). For the preliminary simulations, simple geometric averaging is taken to evaluate the refractive index of the MQW layer and hence its waveguiding properties (Fig. 6). The gain-carrier density relation for the MQWs is taken from [16]. The results (Fig. 7) predict impractically high values of N_{th}, certain to cause prohibitively high threshold currents due to Auger recombination and carrier leakage, for MQW lasers with small values of L, particularly if the higher of the available estimates of σ_h [13] is taken for the MQW structure. In contrast, with bulk active layers such lengths are, not just accessible, but predicted to give the best pulsed performance as shown in Fig. 4. More detailed comparison will be presented at the conference.

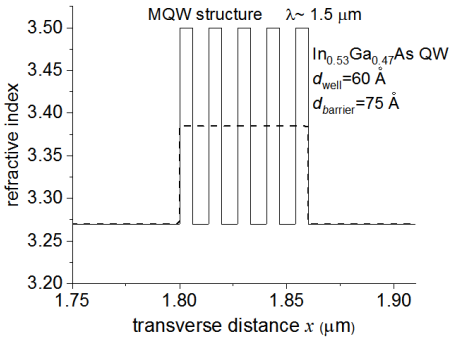

Figure 6. Schematic refractive index profile of the MQW structure and the averaged refractive index profile used in simulations (dashed).

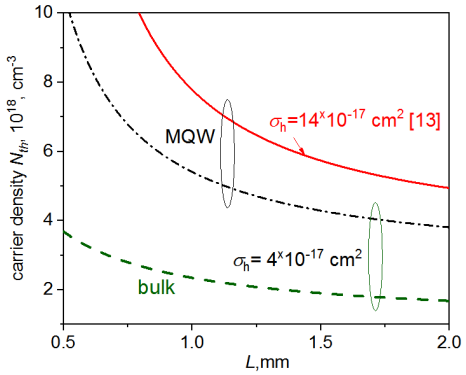

Figure 7. Calculated threshold carrier densities for bulk (as in Fig. 1) and MQW (unstrained InGaAs, as in Fig. 6a) AL structures.

ACKNOWLEDGEMENTS

This work was partly funded by the Academy of Finland under grant 317144.

REFERENCES

[1] V. Molebny, G. Kamerman, and O. Steinvall, "Laser radar: from early history to new trends," in *Proc. SPIE* 7835, 2010, p. 7835023.

[2] B. S. Ryvkin and E. A. Avrutin, "Asymmetric, nonbroadened large optical cavity waveguide structures for high-power long-wavelength semiconductor lasers," *J. Appl. Phys.,* vol. 97, no. 11, p. 123103, Jul. 2005.

[3] J. F. Boucher and J. J. Callahan, "Ultra-high-intensity 1550nm single junction pulsed laser diodes," in *Proc. SPIE* 8039, Orlando, FL, USA, 2011, p. 80390B.

[4] A. A. Marmalyuk, Y. L. Ryaboshtan, P. V. Gorlachuk, M. A. Ladugin, A. A. Padalitsa, S. O. Slipchenko, A. V. Lyutetskiy, D. A. Veselov, and N. A. Pikhtin, "Semiconductor AlGaInAs/InP lasers with ultra-narrow waveguides," *Quantum Electron.*, vol. 47, no. 3, pp. 272–274, Mar. 2017.

[5] T. Tanbun-Ek, Z.Xu, J.Mott, "High power diode laser pump sources in the 1.2-1.9 µm range," in *Proc. 2019 IEEE Conference on High Power Laser Diodes and Systems (HPD)*, Coventry, UK, Sep. 2019, pp. 15-16

[6] P. Crump, G. Erbert, H. Wenzel, C. Frevert, C. M. Schultz, K. H. Hasler, R. Staske, B. Sumpf, A. Maaßdorf, F. Bugge, S. Knigge, and G. Trankle, "Efficient high-power laser diodes," *IEEE J. Sel. Top. Quantum Electron.*, vol. 19, no. 4, p. 1501211, Jul.–Aug. 2013

[7] K. H. Hasler, H. Wenzel, P. Crump, S. Knigge, A. Maasdorf, R. Platz, R. Staske, and G. Erbert, "Comparative theoretical and experimental studies of two designs of high-power diode lasers," *Semicond. Sci. Technol.*, vol. 29, no. 4, p. 045010, Apr. 2014.

[8] B. S. Ryvkin, E. A. Avrutin, and J. T. Kostamovaara, "Strong doping of the *n*-optical confinement layer for increasing output power of high-power pulsed laser diodes in the eye safe wavelength range," *Semicond. Sci. Technol.*, vol. 32, no. 12, p. 125008, Dec. 2017.

[9] L.W. Hallman, B. S. Ryvkin, E. A. Avrutin, A. T. Aho, J. Viheriälä, M. Guina, and J. T. Kostamovaara, "High power 1.5µm pulsed laser diode with asymmetric waveguide and active layer near *p*-cladding", *IEEE Photon. Technol. Lett.*, vol. 31, no. 30, pp. 1635-1638, Oct. 2019

[10] L.W. Hallman, B. S. Ryvkin, E. A. Avrutin, A. T. Aho, J. Viheriälä, M. Guina, and J. T. Kostamovaara, "Double asymmetric structure 1.5µm high power pulsed laser diodes," in *Proc. 2019 IEEE Conference on High Power Laser Diodes and Systems (HPD), Coventry*, UK, Sep. 2019, pp. 19-20.

[11] B. S. Ryvkin, E. A. Avrutin, and J. T. Kostamovaara, "Asymmetric-waveguide, short cavity designs with a bulk active layer for high pulsed power eye-safe spectral range laser diodes", *Semicond. Sci. Technol.*, accepted for publication.

[12] E. A. Avrutin and B. S. Ryvkin, "Theory of direct and indirect effect of two-photon absorption on nonlinear optical losses in high power semiconductor lasers," *Semicond. Sci. Technol,* vol. **32**, no. 1, p. 015004, Jan. 2017.

[13] I. Joindot and J. L. Beylat, "Intervalence band absorption coefficient measurements in bulk layer, strained and unstrained multiquantum well 1.55 µm semiconductor lasers," *Electron. Lett.*, vol. 29, no. 7, pp. 604–606, Apr. 1993.

[14] J. Piprek, "*Semiconductor Optoelectronic Devices: Introduction to Physics and Simulation*," San Diego, CA: Academic Press, 2003.

[15] J. Leuthold, M. Mayer, J. Eckner, G. Guekos, H. Melchior, and C. Zellweger, "Material gain of bulk 1.55 mu m InGaAsP/InP semiconductor optical amplifiers approximated by a polynomial model," *J. Appl. Phys.,* vol. 87, no. 1, pp. 618-620, Jan. 2000.

[16] L. A. Coldren, S. W. Corzine, and M. K. Mashanovitch," *Diode Lasers and Photonic Integrated Circuits*," 2nd ed. NY: Wiley, 2012.